

# Molecular Recognition in Cyclodextrin Complexes of Amino Acid Derivatives. 2.<sup>1</sup> A New Perturbation: The Room-Temperature Crystallographic Structure Determination for the *N*-Acetyl-*p*-methoxy-*L*-phenylalanine Methyl Ester/ $\beta$ -Cyclodextrin Complex

Joanna L. Clark, Billy R. Booth, and John J. Stezowski\*

Contribution from the Department of Chemistry, University of Nebraska—Lincoln, Lincoln, Nebraska 68588-0304

Received January 2, 2001

**Abstract:** Cyclodextrins (CDs) are cyclic oligosaccharides that encapsulate various small organic molecules, forming inclusion complexes. Because CD complexes are held together purely by noncovalent interactions, they function as excellent models for the study of chiral and molecular recognition mechanisms. Recently, room-temperature crystallographic studies of both the 2:2 *N*-acetyl-*L*-phenylalanine methyl ester/ $\beta$ -CD and 2:2 *N*-acetyl-*L*-phenylalanine amide/ $\beta$ -CD complexes were reported. The effect of changes in carboxyl backbone functional group on molecular recognition by the host CD molecule was examined for the nearly isomorphous supramolecular complexes. A new perturbation of the system is now examined, specifically perturbation of the aromatic side chain. We report a room-temperature crystal structure determination for the 2:2 *N*-acetyl-*p*-methoxy-*L*-phenylalanine methyl ester/ $\beta$ -CD inclusion complex. The complex crystallizes isomorphously with the two previously reported examples in space group *P*1; the asymmetric unit consists of a hydrated head-to-head host dimer with two included guest molecules. The crystal packing provides both a nonconstraining extended hydrophobic pocket and an adjacent hydrophilic region, where hydrogen-bonding interactions can potentially occur with primary hydroxyl groups of neighboring CD molecules and waters of hydration. The rigid host molecules show no sign of conformational disorder, and water of hydration molecules exhibit the same type of disorder observed for the other two complexes, with a few significant differences in locations of water molecules in the hydrophilic region near guest molecules. There is evidence for modest disorder in the guest region of an electron density map. In comparing this system with the two previously reported complexes of phenylalanine derivatives, it is found that the packing of the guest molecules inside the torus of the CD changes upon substitution of a methoxy group at the para position of the aromatic phenyl ring. Backbone hydrogen-bonding interactions for the guest molecules with the CD primary hydroxyls and waters also change. This structure determination is a new and revealing addition to a small but growing database of amino acid and peptidomimetic interactions with carbohydrates.

## Introduction

The use of small-molecule crystals for models of molecular recognition in proteins has been recognized as contributing invaluable information about the anchoring of molecules in sterically constrained and unconstrained scaffolds.<sup>2</sup> In the accompanying paper, we report a structural study of two different phenylalanine derivatives complexed with  $\beta$ -CD: *N*-acetyl-*L*-phenylalanine methyl ester (*N*-Ac-*L*-FOMe) and *N*-acetyl-*L*-phenylalanine amide (*N*-Ac-*L*-FNH<sub>2</sub>).<sup>1</sup> In that work, it was found the crystal lattice provided two examples of binding pockets each capable of including molecules of chemically related guest molecules by adapting the hydrogen-bonding interactions with waters and primary hydroxyls to recognize the guest molecules. The host molecules are hydrogen-bonded CD dimers that present the guest molecule with an extended

nonconstraining hydrophobic pocket in which phenylalanine derivatives dock and loosely bind. In addition, intermolecular interactions among the guest molecule backbones, CD primary hydroxyls of neighboring host dimers, and waters were found to play an important role in the mode of penetration and orientation of the guest molecules in the complex. Perturbing the pseudopeptide backbone of the guest molecule by modification of the carboxy terminal residue did not result in extreme changes in the guest binding modes, although an overall shift of the center of mass of the *N*-Ac-*L*-F-NH<sub>2</sub> guest molecules was observed. The shift was likely induced by intermolecular hydrogen-bonding interactions between symmetry-independent amide moieties not possible for the *N*-Ac-*L*-FOMe guest.

Believing that the system presents an unusually interesting model for a systematic study of molecular recognition, we expanded the study to include a chemical modification of the amino acid side chain. The structure of the *N*-acetyl-*p*-methoxy-*L*-phenylalanine methyl ester/ $\beta$ -CD complex (*N*-Ac-*p*-OCH<sub>3</sub>-*L*-FOMe/ $\beta$ -CD) has been determined by room-temperature single-crystal X-ray diffraction analysis. By comparing the intermolecular

\* To whom correspondence should be addressed. E-mail: jstezowski1@unl.edu.

(1) Paper 1 of this series: Clark, J. L.; Stezowski, J. J. *J. Am. Chem. Soc.*, preceding paper in this issue.

(2) Czugler, M. *J. Mol. Recognit.* 1993, 6, 187–194.

interactions in this new complex with the previously reported amino acid derivative complexes, we expect to gain more understanding of the importance of guest molecule steric requirements and amino acid side-chain functional groups to the process of molecular recognition by the CD.

### Experimental Section

The complex was prepared by combining a 1:1 molar ratio of  $\beta$ -CD (Cerestar) with *N*-Ac-*p*-OCH<sub>3</sub>-L-FOMe (Bachem) in aqueous solution and heating gently. In  $\sim$ 24 h, platelike parallelepiped microcrystals of the complex appeared. The solution was filtered, and larger crystals were grown from the filtrate by slow evaporation at room temperature. A  $0.4 \times 0.3 \times 0.1$  mm<sup>3</sup> parallelepiped single crystal was sealed in a thin-walled glass capillary with mother liquor for data collection. Room-temperature diffraction data were measured using a Bruker AXS molybdenum target rotating anode X-ray source (50 kV/90 mA) and an 18-cm MARresearch image plate detector. Lattice parameters,  $a = 18.30(6)$ ,  $b = 15.50(6)$  and  $c = 15.31(6)$  Å,  $\alpha = 102.77(6)^\circ$ ,  $\beta = 112.66(6)^\circ$ ,  $\gamma = 99.47(6)^\circ$ , and  $V = 3756.9$  Å<sup>3</sup>, were determined from spot centroids from the imaging plate. A total of 24 645 reflections of which 12 425 are unique reflections were collected by the oscillation method,  $R(\text{int}) = 0.0395$ , to a resolution of 0.86 Å. The MARXDS program was used to process the data.<sup>3</sup> Isomorphous replacement of the  $\beta$ -CD coordinates from the *N*-Ac-L-FOMe complex<sup>1</sup> resulted in a solution to the phase problem. The chemical formula was found to be  $2\text{C}_{42}\text{H}_{70}\text{O}_{35} \cdot 2\text{C}_{13}\text{H}_{17}\text{O}_4\text{N}_1 \cdot 21.85\text{H}_2\text{O}$ . Least-squares refinement on  $F^2$  was carried out for 1639 parameters and 31 restraints using SHELXL97<sup>4</sup> and converged to a final  $R_1 = 0.0832$ ,  $wR_2 = 0.2273$ , and GOF = 1.029 for 10 035 reflections with  $F_o = 4\sigma(F_o)$ . For the cyclodextrin, all non-hydrogen atoms were refined anisotropically. Hydrogens on carbons were generated geometrically and included using a riding model.

Waters of hydration were located in difference electron density maps ( $F_o - F_c$ ). Seven well-ordered waters were refined with anisotropic ADPs, and 14.85 disordered waters distributed over 35 sites were refined isotropically. The X-ray data reveal minor evidence for disorder in the guest region of electron density, Figure 1. The electron density around some of the atoms has a significantly nonspherical appearance, which could indicate some libration (thermal motion) or static disorder. Initially only two guest molecules were incorporated to model the electron density; however, at very low electron density levels ( $<0.4$  e<sup>-</sup>/Å<sup>3</sup>), evidence for another ring conformation was observed in the **B** monomer. It was not possible to adequately model the density as a separate ring conformation alone; in addition, there were some low residual peaks located near the backbone area of the guest molecule. Because of this, an entirely new guest (**B2**) with an estimated 20% population parameter was included in the model to account for the disorder. Residual electron density was also observed near the ester moiety of the guest molecule in monomer **A**, which required modeling two ester backbone sites, with 75% and 25% estimated populations.

In monomer **B**, the two distinct guest molecules were refined differently. The more highly populated guest was allowed to refine with isotropic ADPs, while the guest molecule with the lower population was refined with a single group isotropic ADP. In the other monomer (**A**), the two distinct ester sites were refined with group isotropic ADPs. A final ( $F_o - F_c$ ) map showed  $\rho_{\text{max}} = 0.67$ ,  $\rho_{\text{min}} = -0.55$ . Crystallographic data in cif format are available. Hydrogen-bonding interactions were analyzed using the Parst97 program.<sup>5</sup>

### Results and Discussion

In Figure 2, the unit cell contents are illustrated in a stereoscopic projection; a similar plot with refined thermal ellipsoids presented for all C, N, and O atoms at the 50% probability level has been deposited. The complex crystallizes with space group symmetry *P1* and is nearly isomorphous with

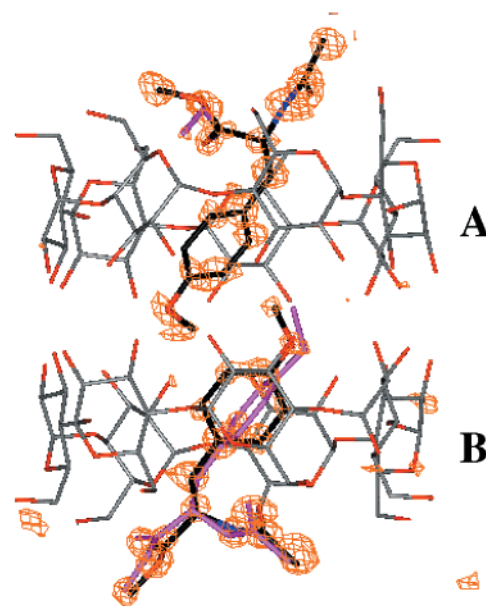


**Figure 1.** Difference electron density map with the guest omitted from the structure factor calculation superimposed over the modeled guests for the 2:2 *N*-Ac-*p*-OCH<sub>3</sub>-L-phenylalanine methyl ester/ $\beta$ -cyclodextrin complex. Hydrogen atoms on the CD and guests as well as waters are omitted for clarity. The electron density level is  $0.45$  e<sup>-</sup>/Å<sup>3</sup>. The nature of the electron density indicates modest disorder in the guest region. The guests shown colored by atom type, with black carbon atoms, blue nitrogen atoms, and red oxygen atoms, are the most highly populated. The guests or backbone regions shown in magenta have lower populations. The CD dimer is shown colored by atom type, with gray carbon atoms and red oxygen atoms.

those reported in the accompanying report for the *N*-Ac-L-phenylalanine methyl ester and amide complexes. The asymmetric unit consists of a head-to-head hydrogen-bonded  $\beta$ -CD dimer,  $\sim$ 22 waters of hydration, and two included guest molecules. The disorder in the guest molecules discussed above is color-coded (the major component in each host monomer is blue). The nearly isomorphous nature of these crystal structures supports the use of this series of complexes as models for molecular recognition, by providing very similar lattice-packing contributions that give rise to a common environment (binding pocket; see the accompanying report for an illustration) for docking small bioorganic molecules.

In the discussion to follow, we compare the structure for the *N*-Ac-*p*-OCH<sub>3</sub>-L-FOMe/ $\beta$ -CD complex with those for the two other previously reported isomorphous complexes: the *N*-Ac-L-FOMe/ $\beta$ -CD complex and the *N*-Ac-L-FNH<sub>2</sub>/ $\beta$ -CD complex.<sup>1</sup> Differences and similarities in the three complexes provide a more complete picture of molecular recognition. Figure 2 is helpful in defining the monomers **A** and **B** that associate to form the  $\beta$ -CD dimer. These monomers are referred to frequently in the following discussion. (See the accompanying paper<sup>1</sup> for a description of the atom-labeling scheme.)

The host structure of the *N*-Ac-*p*-OCH<sub>3</sub>-L-FOMe/ $\beta$ -CD complex was described above as a conformationally rigid molecule. In contrast to both the *N*-Ac-L-FOMe and the *N*-Ac-L-FNH<sub>2</sub> complexes, where primary hydroxyls O6(1) and O6(5) are disordered over two sites, disorder is not observed for any of the primary hydroxyls in this system. Primary hydroxyl O6(1) is observed in a (+)-gauche conformation, where the hydroxyl points toward the interior of the CD torus, while all other primary hydroxyls are observed in the more common (-)-gauche conformation. None of the primary hydroxyls show signs of significant librational averaging. As observed for the other

(3) Kabsch, W. *J. Appl. Crystallogr.* **1988**, *21*, 916–924.

(4) Sheldrick, G. M. *SHELXL97. Program for the Refinement of Crystal Structures*; University of Göttingen, Germany, 1997.

(5) Nardelli, M. *Comput. Chem.* **1983**, *7*, 95–98

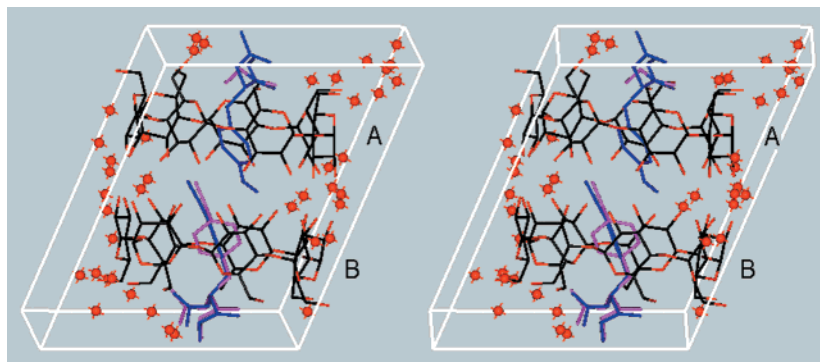


**Figure 2.** Contents of one unit cell for the *N*-Ac-*p*-OCH<sub>3</sub>-L-FOMe complex. The disordered included molecules are color-coded: the more highly occupied molecule is blue. See the text for a discussion of the relative populations. The CD is colored in the same manner as Figure 1.

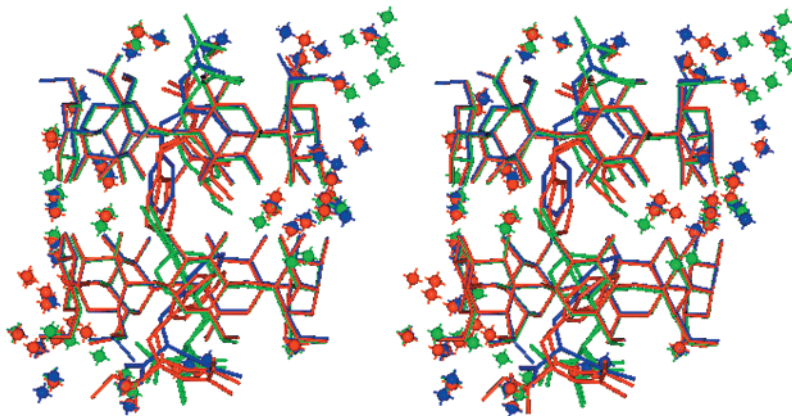


**Figure 3.** Color-coded stereoscopic superposition diagram of the contents of one unit cell for the three  $\beta$ -CD complexes of phenylalanine derivatives studied so far: the *N*-Ac-L-FOMe/ $\beta$ -complex (blue), the *N*-Ac-L-FONH<sub>2</sub> complex (red), and the *N*-Ac-*p*-OCH<sub>3</sub>-L-FOMe complex (green). The figure supports comparison of the guest positions, conformations, and orientations inside the CD dimer and the positions of water of hydration molecules in the three structures. Note the similarities of the cyclodextrin conformation; the only significant difference being the presence or absence of a small number of disordered primary hydroxyl groups.

two nearly isomorphous complexes, there are five interdimer hydrogen bonds between primary hydroxyls, four of which are intrasheet. The fifth contact is intersheet, which aids in stabilizing the Im packing arrangement.

Several water of hydration molecules are located in pockets between CD dimers. These space-filling waters are disordered in a manner that is common to most CD complexes and are probably bound only loosely in the crystal. Many of the waters occupy split positions, and several hydrogen-bonding interactions with various primary and secondary hydroxyls of the CDs occur. Comparing the *N*-Ac-*p*-OCH<sub>3</sub>-L-FOMe complex with the *N*-Ac-L-FOMe complex reveals some differences in water structure and location, especially in the dimer interface region, where guest molecule backbones are typically located. Two water molecules previously observed in the other two complexes, w26 and w39, are not observed in the *N*-Ac-*p*-OCH<sub>3</sub>-L-FOMe complex. Instead, a new water location, w61, is observed, along with a new distribution of disordered w29's, with a sum total occupancy larger than 1.00. We discuss the interactions involving w29 and w61 later in conjunction with guest hydrogen-bonding interactions; they interact significantly with the guest molecules in the **B** monomer.

The positions and orientations of the guest molecules have changed significantly compared to those in the previously reported complexes. Similarities and differences in the three structures can be assessed using the color-coded, stereoscopic superposition diagram of the contents of one unit cell, presented in Figure 3. While the host and water structures are clearly very similar for all three complexes, there are interesting differences

in guest positions, conformations, and orientations. Some disordered water molecules with split positions appear close together in the drawing. Figure 4 is a simplified comparison of the positions and orientations of the different guest molecules in the three complexes. Various arrows and scales appear on this figure; the utility of these notations will be discussed below. Only one pair of guest sites, the most highly populated pair, is presented for each complex; the CD dimers are illustrated in the same orientation.

Comparison of the structures illustrated in Figures 3 and 4 reveals that substituting a methoxy group in the para position onto the aromatic ring produces a number of interesting changes in the molecular interactions in the complex and in the binding pockets provided by the crystal lattice. For example, it alters the depth of penetration of the guest molecules in the hydrophilic interface between sheets. To accommodate the larger methoxy-substituted ring, the side chains of the *N*-Ac-*p*-OCH<sub>3</sub>-L-FOMe guests occupy more of the volume of the extended torus of the CD dimer. As a result, the positions, orientations, and conformations of the *N*-Ac-*p*-OCH<sub>3</sub>-L-FOMe guest molecules are different from those of the parent *N*-Ac-L-FOMe guest molecules. The conformation of the *N*-Ac-*p*-OCH<sub>3</sub>-L-FOMe guest in monomer **A** places the ester moiety near the exterior of the CD torus, unlike that of the **A** monomer *N*-Ac-L-FOMe guest, in which the ester is tucked into the torus and located near the secondary hydroxyls. The *p*-methoxy **A** guest has both a backbone position and orientation more similar to that of the *N*-Ac-L-FNH<sub>2</sub> guest molecule. Although the guest conformations for the *N*-Ac-*p*-OCH<sub>3</sub>-L-FOMe and *N*-Ac-L-FNH<sub>2</sub> guests are not



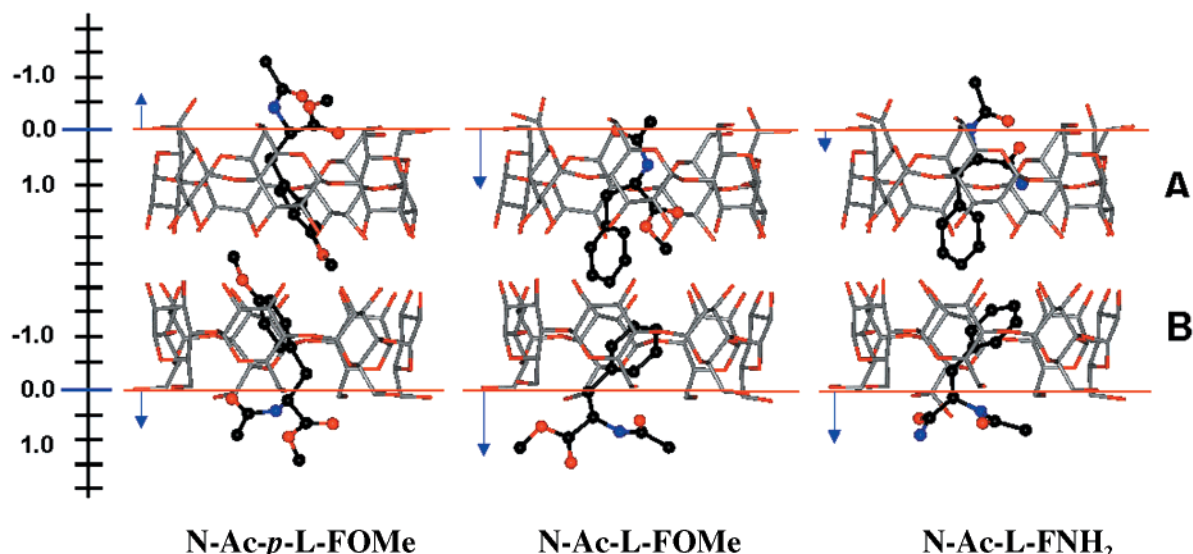


**Figure 4.** Side-by-side comparison of the three  $\beta$ -CD complexes of phenylalanine derivatives studied so far. Only the most highly populated guest molecules or one guest molecule of an equally disordered pair is illustrated for clarity. This figure illustrates the differences in positions and orientations of the guest molecules in the CD torus (gray). The calculations of backbone COMs are also shown on this figure. The tip of the red arrow indicates an approximate distance of the backbone midpoint from the appropriate calculated mean C6 plane and also the directionality of the shift. A scale is provided on the left for quantifying the shifts. Guest molecules are colored by atom type, with black carbon atoms, blue nitrogen atoms, and red oxygen atoms.

**Table 1.** Torsions Angles (deg) Characterizing the *N*-Ac-*p*-OCH<sub>3</sub>-L-FOMe Guest Conformations

torsion angle	A(ester 1)*	A(ester 2) <sup>a</sup>	B1	B2
$\omega$	173.16	-173.16	154.57	171.43
$\phi$	-85.88	-85.88	-117.38	128.17
$\varphi$	-32.88	-55.04	88.46	74.25
$\chi_1$	166.49	166.49	-64.17	-75.15
$\chi_2$	78.06	78.06	70.94	167.80
$\eta^b$	37.21	37.21	15.68	114.21

<sup>a</sup> Ester sites 1 and 2 for the **A** guest are shown in Figure 1. <sup>b</sup> Torsion angle describing-OCH<sub>3</sub> conformation.

identical, the acetyl backbone conformations are very similar. Table 1 lists torsion angles for the *N*-Ac-*p*-OCH<sub>3</sub>-L-FOMe guests.

The two disordered *N*-Ac-*p*-OCH<sub>3</sub>-L-FOMe guests in monomer **B** are significantly different in conformation, position, and orientation from the guests in either of the other two complexes. The aromatic rings are oriented differently, and the ester backbones are located in virtually the opposite location from that observed for the *N*-Ac-L-FOMe guest molecule. Both hydrogen-bonding interactions, which are discussed later, and spatial considerations may be responsible for this large change in the guest position in monomer **B**.

The addition of the methoxy substituent onto the aromatic ring of the *N*-Ac-L-FOMe molecule was expected to affect the packing of the two guests inside the  $\beta$ -CD dimer. In the *N*-Ac-L-FOMe and *N*-Ac-L-FNH<sub>2</sub> complexes, the aromatic rings in monomers **A** and **B** experience at least weak C-H- $\pi$  interactions. The distances calculated between aromatic ring centroid pairs range from 4.68 to 4.83 Å. The distances between aromatic ring centroid pairs for the *p*-methoxy-substituted guests are 5.53 (from guest **A** to **B1**) and 5.64 Å (from guest **A** to **B2**). This comparison and the differences in ring positions and orientations indicate that the aromatic ring packing interactions previously observed for the *N*-Ac-L-FOMe guests are not present for the *N*-Ac-*p*-OCH<sub>3</sub>-L-FOMe guests. Figure 4 further illustrates this point; the aromatic rings in the *N*-Ac-*p*-OCH<sub>3</sub>-L-FOMe complex do not appear to interact in either edge-to-face or parallel-stacked arrangements. Increasing the size and steric character of the side

**Table 2.** Parameters for Hydrogen-Bonding Interactions Observed in the *N*-Ac-*p*-OCH<sub>3</sub>-L-FOMe/ $\beta$ -CD Complex

interaction	distance (heavy atom to heavy atom) (Å)	populations (%) atom 1:atom 2
w29b--Oes(B1) ( $x-1,y,z$ )	2.76(4)	50:75
w29b--Oes(B2) ( $x-1,y,z$ )	3.12(4)	50:25
w61--N(B1) ( $x-1,y,z$ )	3.10(1)	100:80
w61--N(B2) ( $x-1,y,z$ )	3.22(1)	100:20
O6(3)--w29b ( $x,y,z-1$ )	2.78(3)	100:50
O6(3)--w29a ( $x,y,z-1$ )	2.66(1)	100:40
w29b--w61	2.62(4)	50:100
O6(5)--w61	2.78(2)	100:100
O6(2)--w61 ( $x,y,z-1$ )	2.78(1)	100:100
O6(2)--O6(6) ( $x,y,z-1$ )	2.79(1)	100:100
O6(6)--w16	2.76(1)	100:100
w16--w38c ( $x-1,y,z$ )	2.89(2)	100:65
w16--w24 ( $x,y+1,z$ )	2.80(2)	100:100
W16--O6(10) ( $x-1,y-1,z$ )	2.79(1)	100:100
w38c--OAc(A) ( $x-1,y,z$ )	2.77(2)	65:100
NAc(A)--w31a	3.00(1)	100:60
w31a--O6(8) ( $x-1,y,z-1$ )	3.04(2)	60:100
w31a--w19 ( $x-1,y,z-1$ )	2.87(1)	60:100
O6(12)--w31a ( $x+1,y,z$ )	3.68(2)	100:60
w19--w18 ( $x,y,z+1$ )	2.76(2)	100:100
O6(12)--w18	2.78(1)	100:100
w18--w44a ( $x,y,z-1$ )	2.71(6)	100:60
w18--w32y	2.99(5)	100:50
O6(12)--O6(8) ( $x,y,z-1$ )	2.97(1)	100:100
O6(8)--w17 ( $x,y,z+1$ )	2.68(1)	100:100
w17--O6(11)	2.71(2)	100:100
w17--w33 ( $x+1,y,z$ )	2.86(1)	100:100
w33--O6(9) ( $x-1,y,z-1$ )	2.70(1)	100:100
O6(1)--w19 ( $x-1,y,z-1$ )	2.77(1)	100:100
w19--O6(14)	2.72(1)	100:100
O6(1)--O6(9) ( $x-1,y-1,z-1$ )	2.73(1)	100:100
O6(4)--O6(7) ( $x,y+1,z$ )	2.83(1)	100:100
O6(10)--O6(14) ( $x,y+1,z$ )	2.78(1)	100:100

chain has removed the C-H- $\pi$  interaction between the aromatic rings. Instead of packing in the torus in an edge-to-face manner, the *N*-Ac-*p*-OCH<sub>3</sub>-L-FOMe guests pack with the methyl functional group of the methoxy substituents located near the aromatic ring of the opposite guest molecule in the dimer. This

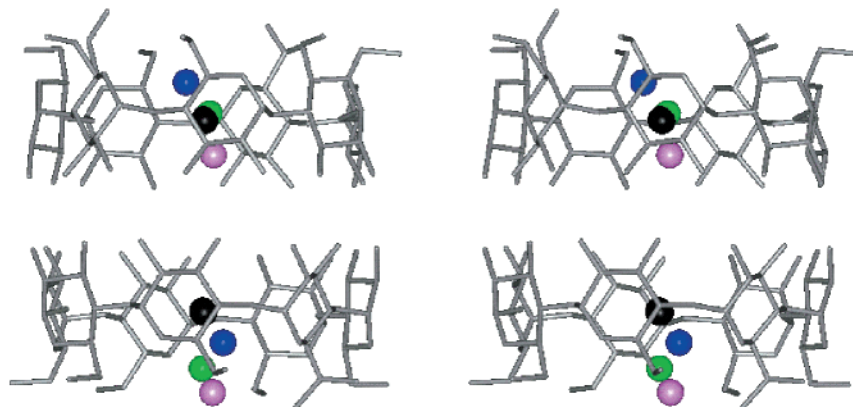


**Figure 5.** Color-coded stereoscopic representation of the calculated approximate centers of mass for the guest molecules in the three complexes reported so far. The black spheres represent the midpoints of the CD O4 atoms for that particular monomer. The others spheres: blue, *N-Ac-p-OCH<sub>3</sub>-L-FOMe* guest midpoint; magenta, *N-Ac-L-FOMe* guest midpoint; and cyan, *N-Ac-L-FNH<sub>2</sub>* guest midpoint. The figure shows that the *N-Ac-p-OCH<sub>3</sub>-L-FOMe* guests are both shifted some distance from the calculated O4 midpoints, toward the hydrophilic interdimer space. In contrast, the other two sets of guest midpoints (*N-Ac-L-FOMe*, *N-Ac-L-FNH<sub>2</sub>*) shift in a concerted direction, toward the B monomer along the **a** cell axis direction.

arrangement is not entirely unexpected; the methoxy group is relatively nonpolar and could be expected to experience favorable van der Waals interactions with the aromatic ring of a nearby guest. The intermolecular contact distances between the methyl carbon of the guest in **A** and the centroids of the aromatic rings of guests **B1** and **B2** are 3.89 and 3.96 Å, respectively. The distances from the methyl carbon of guests **B1** and **B2** to the centroid of guest **A** are 3.80 and 3.87 Å. These distances are consistent with van der Waals close contacts between the  $\pi$  density of an aromatic ring and a methyl carbon atom. The oxygen atom of guest **A**'s methoxy substituent is located at distances of 4.33 and 4.48 Å from the opposite guest aromatic ring centroids of **B1** and **B2**. The methoxy oxygens of guests **B1** and **B2** are located a distance of 4.49 and 4.57 Å away from the centroid of the **A** guest aromatic ring.

When comparing the positions of the guest molecules in the three complexes, shifts of the different guest molecules inside the torus are particularly useful. It was previously reported that the average midpoints of the aromatic rings of guest molecules in the *N-Ac-L-FNH<sub>2</sub>* and *N-Ac-L-FOMe* complexes are shifted overall with respect to their positions in the torus; the *N-Ac-L-FNH<sub>2</sub>* guest pair is displaced by  $\sim 0.985$  Å toward the torus center from the position of the *N-Ac-L-FOMe* methyl ester guest pair. The *N-Ac-p-OCH<sub>3</sub>-L-FOMe* guest molecules are positioned differently compared to the other previously reported guests; however, due to the reorientation of the aromatic ring moiety in the monomer **B** *N-Ac-L-FOMe* guest, it becomes more difficult to characterize the differences. Because of this, we have developed an improved method for examining differences in guest molecule penetration in the CD torus. The calculation compares the midpoint of the O4 coordinates in each CD monomer, with an estimated guest molecule center of mass (COM) calculated by averaging the atomic coordinates of the guest molecule C, N, and O atoms. The results visually, Figure 5, illustrate the differences in location of the guest molecules.

In monomer **A**, the COM of the *N-Ac-L-FOMe* guest is located 1.35 Å below the O4 midpoint, indicating that this guest molecule is included more completely in the CD torus than any of the other guest molecules. The COM for the **A** *N-Ac-L-FNH<sub>2</sub>* guest is located 0.32 Å above the O4 midpoint, whereas that for the *N-Ac-p-OCH<sub>3</sub>-L-FOMe* **A** guest is 1.58 Å above the respective O4 midpoint; that is, the guest molecule is displaced even further toward the hydrophilic interface. The monomer **B** guests COMs are all located "below" the O4 atom midpoint

for the host; that is, molecules are positioned toward the hydrophilic interface of the dimer; the magnitudes of the shifts vary. Located 3.09 Å from the O4 midpoint, the **B** *N-Ac-L-FOMe* COM displays the largest displacement from the O4 midpoint. The **B** *N-Ac-L-FNH<sub>2</sub>* COM is displaced 2.18 Å from the respective O4 midpoint, while the smallest displacement, 1.32 Å, is found for the *N-Ac-p-OCH<sub>3</sub>-L-FOMe* **B** guest. The COM comparisons are particularly useful when looked at as pairs of COMs, allowing the behavior of the guest pairs to be contrasted. The **A** and **B** *N-Ac-p-OCH<sub>3</sub>-L-FOMe* midpoints appear to be balanced with respect to the O4 midpoints. Each guest is shifted toward its respective hydrophilic interface. In contrast, the guest pairs in the *N-Ac-L-FNH<sub>2</sub>* and *N-Ac-L-FOMe* complexes are shifted toward the **B** monomer.

The differences in the guest arrangements for the three complexes can be attributed to a combination of hydrophobic contacts between guest molecules in the host dimer and interactions in the hydrophilic interface. Aromatic edge-to-face C–H– $\pi$  interactions within guest pairs in the *N-Ac-L-FNH<sub>2</sub>* and *N-Ac-L-FOMe* complexes very likely determine the contact distances between the guest molecules. In the *N-Ac-p-OCH<sub>3</sub>-L-FOMe* complex, the hydrophobic interaction between the methoxy groups and the phenyl rings determines the guest–guest contact distances. Once the contacts within the pair are established, the position of the guest molecules appears to be determined largely by hydrogen-bonding interactions in the hydrophilic interface at both ends of the dimer.

A calculation of the mean backbone locations for the different guest molecules in the three complexes complements the above observations by providing additional insight into the nature of the interactions responsible for molecular recognition. For the monomer **A** guest molecules in the *N-Ac-L-FOMe* and *N-Ac-L-FNH<sub>2</sub>* complexes, the ester and amide moieties of the backbone are included in the interior of the CD torus and the acetyl moiety penetrates the hydrophilic interface only to a modest extent. In contrast, the backbone of the *N-Ac-p-OCH<sub>3</sub>-L-FOMe* **A** guest is located almost entirely in the hydrophobic interface region. To quantify these observations, mean planes were calculated through the C6 atoms (the methylene carbons bonded to the primary hydroxyls) for each host monomer to define a boundary between the hydrophobic torus and the hydrophilic interface. In addition, an approximate center of mass for the backbone atoms was calculated from the coordinates of the non-hydrogen atoms of the pseudopeptide backbone. The

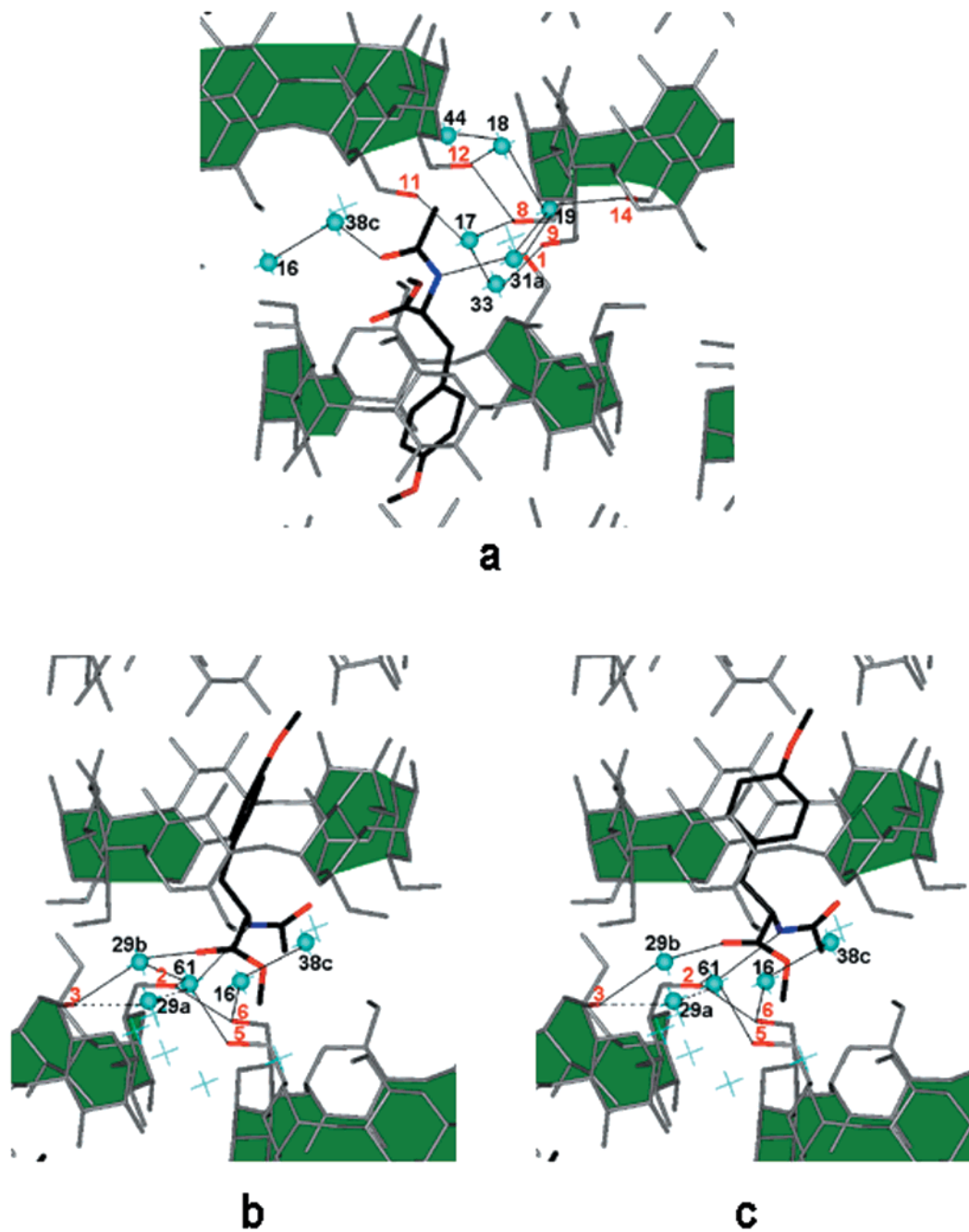


**Figure 6.** Possible hydrogen-bonding interactions for the *N*-acetyl-*p*-OCH<sub>3</sub>-L-phenylalanine methyl ester/ $\beta$ -cyclodextrin complex. The figure is constructed in the same manner as those reported for the *N*-Ac-L-FOMe/ $\beta$ -complex and the *N*-Ac-L-FONH<sub>2</sub> complex.<sup>1</sup> Figure 5a presents the hydrogen-bonding interactions for the molecule in the A pocket. Note that the disorder in the phenyl ring of the side chain for the guest molecule in the B pocket, Figure 5b and c, does not affect the hydrogen-bonding interaction of this guest with the lattice binding pocket. Waters are colored cyan and labeled in black; primary hydroxyls are colored and labeled in red. Guest molecules are colored by atom type, with black carbon atoms, blue nitrogen atoms, and red oxygen atoms. The CD dimer is shown in gray.

distances from these COMs to their corresponding C6 mean plane are illustrated in Figure 5. The red lines in the figure illustrate the C6 mean planes; the red arrow shown to the left of each complex and the associated scale shown illustrate the magnitudes and direction of backbone COM shift from the respective C6 planes. In monomer A, the *N*-Ac-L-FOMe backbone COM penetrates the hydrophobic torus by 2.65 Å. The A *N*-Ac-L-FNH<sub>2</sub> backbone COM penetrates the torus to a lesser extent by 0.50 Å. In contrast, the A *N*-Ac-*p*-OCH<sub>3</sub>-L-FOMe backbone COM penetrates the hydrophilic interface by 0.89 Å. In the B monomer, the backbones of the different guest molecules in all three complexes penetrate the respective hydrophilic interface: *N*-Ac-L-FOMe backbone COM by 1.99

Å, *N*-Ac-L-FNH<sub>2</sub> backbone COM by 1.41 Å, and *N*-Ac-*p*-OCH<sub>3</sub>-L-FOMe by 1.02 Å. We suggest that hydrogen-bonding interactions, discussed below, are primarily responsible for these effects.

Intermolecular hydrogen-bonding interactions between the guest molecules, CD primary hydroxyls and waters occur in the hydrophilic region of interdimer space Table 2. Figure 6 displays the hydrogen-bonding interactions for the three *N*-Ac-*p*-OCH<sub>3</sub>-L-FOMe guest molecules. As observed for the two complexes described in the accompanying report, there are two intermolecular hydrogen bonds between cyclodextrin primary hydroxyls (O6(2)⋯O6(6) and O6(8)⋯O6(12)). The interactions between these hydroxyls form the scaffold for the binding areas



in the Im crystal packing arrangement; however, these four hydroxyl groups do not interact directly with the guest molecules. Primary hydroxyls O6(2) and O6(6) are associated with interactions in the monomer **B** pocket, Figure 6b and 6c, while primary hydroxyls O6(8) and O6(12) are associated with interactions in the **A** pocket, Figure 6a. In **A**, additional primary hydroxyls involved in interactions with waters of hydration are O6(9), O6(11), O6(1), and O6(14). These interactions are illustrated in Figure 6a. The **B** pocket is defined by two other primary hydroxyls that possibly interact with waters of hydration or guest molecules: O6(5) and O6(3).

In the previous study of phenylalanine derivative complexes, the hydrogen-bonding interactions observed in monomer **A** were very similar. The acetyl backbone on the guests can serve either as a hydrogen donor (amide nitrogen) or as a hydrogen acceptor (carbonyl oxygen). For the *N*-Ac-L-FOMe complex, the acetyl oxygen of the guest in monomer **A** served as proton acceptor in a hydrogen-bonding interaction with water w31. In contrast, the amide nitrogen of the *N*-Ac-L-FNH<sub>2</sub> guest in monomer **A** served as a hydrogen donor in an interaction with w31. The *N*-Ac-*p*-OCH<sub>3</sub>-L-FOMe guest in **A** interacts with w31 in the same manner as the *N*-Ac-L-FNH<sub>2</sub> guest molecule, with the amide nitrogen oriented such that it serves as the hydrogen donor to w31. An additional stabilizing interaction is observed; the acetyl oxygen of the *N*-Ac-*p*-OCH<sub>3</sub>-L-FOMe guest interacts with water w38c. Water w38c in turn interacts via w16 with the primary hydroxyl O6(6). Primary hydroxyl O6(6) is one of the primary hydroxyls mentioned above, because it helps define the monomer **B** binding pocket. The ester moiety of the guest in **A** does not appear to participate in any hydrogen-bonding interactions, which is not unusual for this functional group. In the *N*-Ac-L-FOMe complex, the ester moieties were not utilized extensively in hydrogen-bonding interactions.

Because they are very different from any interactions previously observed, hydrogen-bonding interactions that take place near the **B** pocket are perhaps the most notable. The two disordered guests in monomer **B** have remarkably different backbone conformations and positions compared to those of the *N*-Ac-L-FOMe guest molecules in **B**. The result is an entirely new scheme for hydrogen-bonding interactions. The interaction between the guest acetyl oxygen and O6(2), previously observed in both of the other complexes, is no longer present. Water molecules w39 and w26, previously observed to interact with the amide nitrogen on the guest molecules in the other two complexes, are no longer present. Instead, the amide nitrogen of the *N*-Ac-*p*-OCH<sub>3</sub>-L-FOMe guests interacts with a new water molecule, w61. Water w61, which is completely ordered, also interacts with primary hydroxyls O6(5) and O6(2) and disordered water w29b or w29a. Water w29b in turn interacts with the ester carbonyl oxygen of the *N*-Ac-*p*-OCH<sub>3</sub>-L-FOMe guest molecules, as well as primary hydroxyl O6(3). In the *p*-methoxy complex, water w29 has more disordered sites and a higher sum total population than observed in the other two complexes. The presence of the entirely new water position (w61, located 3.92 and 4.33 Å from w39a and w39b) nicely illustrates the role

that water molecules can play in facilitating the binding of similar substrate molecules in a binding pocket with a defined framework.

## Conclusions

The inclusion of the *N*-Ac-*p*-OCH<sub>3</sub>-L-FOMe/ $\beta$ -CD to our earlier study of the complexes with *N*-Ac-L-FOMe and *N*-Ac-L-FNH<sub>2</sub> has provided additional insight into the role of various intermolecular interactions involved in molecular recognition in these crystalline supramolecular complexes. The fact that these complexes are nearly isomorphous indicates that crystal packing, especially direct and water-mediated interactions between sheets of  $\beta$ -CD dimers, provides a framework for the binding pockets. Also, on the basis of the observations of the positions and orientations of the aromatic rings in the three complexes, we suggest that hydrophobic interactions in the form of close contacts between atoms of the side chains determine how far the pseudopeptide backbones protrude from the host torus into the hydrophilic interface. Finally, it can be concluded that conformations of the pseudopeptide backbones and their orientations with respect to the side chains are largely determined by water-mediated hydrogen-bonding interactions between the guest molecules and the binding pocket frameworks described above.

We suggest that this system provides an especially good model for the study of molecular recognition at atomic resolution. The binding pocket framework serves as a model for a macromolecular receptor with one or more recognition sites (e.g., hydrogen bond donors and/or acceptors) with modest conformational flexibility (rotation about hydroxyl C–O bonds). Like many biological receptors, water molecules play a role in mediating host–substrate recognition. Similarly, conformational flexibility in the substrate molecule is utilized to achieve effective binding between the host and substrate.

As the database of structures determined for amino acid/ $\beta$ -CD complexes grows, an even better understanding of the interrelationship between steric effects and weak binding interactions will be gained. The results of such structure determinations are expected to serve as an experimental basis for molecular modeling calculations designed to provide a better understanding of the thermodynamics of substrate–receptor binding. The fact that disorder in the conformations, orientations, and positions of the guest molecules is observed in the supramolecular complexes will provide a number of energetically similar starting models for such calculations.

**Acknowledgment.** This work was supported in part by the NSF (CHE-9812146).

**Supporting Information Available:** CIF data, an ORTEP plot illustrating refined atomic displacement parameters. This material is available free of charge via the Internet at <http://pubs.acs.org> JA0100221. See any current masthead page for ordering information and Web access instructions.

JA0100221